

LA-UR-11-10356

Approved for public release; distribution is unlimited.

Title: Full-waveform inversion in the time domain with an energy-weighted gradient

Author(s):
Zhang, Zhigang
Huang, Lianjie
Lin, Youzuo

Intended for: 81st SEG Annual Meeting, 2011-09-18/2011-09-23 (San Antonio, Texas, United States)



Disclaimer:

Los Alamos National Laboratory, an affirmative action/equal opportunity employer, is operated by the Los Alamos National Security, LLC for the National Nuclear Security Administration of the U.S. Department of Energy under contract DE-AC52-06NA25396. By acceptance of this article, the publisher recognizes that the U.S. Government retains nonexclusive, royalty-free license to publish or reproduce the published form of this contribution, or to allow others to do so, for U.S. Government purposes.

Los Alamos National Laboratory requests that the publisher identify this article as work performed under the auspices of the U.S. Department of Energy. Los Alamos National Laboratory strongly supports academic freedom and a researcher's right to publish; as an institution, however, the Laboratory does not endorse the viewpoint of a publication or guarantee its technical correctness.

Full-waveform inversion in the time domain with an energy-weighted gradient

Zhigang Zhang, Youzuo Lin and Lianjie Huang, Los Alamos National Laboratory, Geophysics Group, MS D443, Los Alamos, NM 87545

SUMMARY

When applying full-waveform inversion to surface seismic reflection data, one difficulty is that the deep region of the model is usually not reconstructed as well as the shallow region. We develop an energy-weighted gradient method for the time-domain full-waveform inversion to accelerate the convergence rate and improve reconstruction of the entire model without increasing the computational cost. Three different methods can alleviate the problem of poor reconstruction in the deep region of the model: the layer stripping, depth-weighting and pseudo-Hessian schemes. The first two approaches need to subjectively choose stripping depths and weighting functions. The third one scales the gradient with only the forward propagation wavefields from sources. However, the Hessian depends on wavefields from both sources and receivers. Our new energy-weighted method makes use of the energies of both forward and backward propagated wavefields from sources and receivers as weights to compute the gradient. We compare the reconstruction of our new method with those of the conjugate gradient and pseudo-Hessian methods, and demonstrate that our new method significantly improves the reconstruction of both the shallow and deep regions of the model.

INTRODUCTION

Surface seismic surveys are most commonly used in energy exploration and reservoir monitoring. Full-waveform inversion is becoming a promising tool for velocity updating with increasing computing powers. However, full-waveform inversion of surface seismic reflection data usually reconstructs the shallow region of the velocity model better than the deeper region. It has been recognized that this phenomenon is caused by the uneven spatial distribution of seismic energy in the model. The dominant effect causing this uneven distribution is the geometrical spreading and therefore, the shallow region is better resolved than the deep region when both sources and receivers are located on the surface.

Three different methods have been developed to alleviate the problem of poor reconstructions in the deep region of the model. The layer stripping method updates the shallow region of the model or the entire model first (Wang and Rao, 2009), and then updates the deep region. It may consist of several starting depths that gradually moves downward. Because the magnitude of the gradient is larger in the shallow region than that in the deep region of the model, the shallow region reaches the best-fit model earlier than the deep region. So the layer stripping method can improve the reconstruction of the deep region of the model. Another method is the depth-weighting method that amplifies the gradient in the deep region by multiplying the gradient with a function of depth. It balances the magnitude of the gradient by giving more weight to the deep region

(Wang and Rao, 2009; Brenders and Pratt, 2007). These two methods are helpful to improve reconstruction images. However, the decay of the gradient is not strictly a function of the depth, and there are no objective criteria to implement the layer stripping and depth-weighting methods. For example, in the layer stripping method, when and where to move to the next stripping depth level are rather subjective during implementation. Different choices may not lead to the same result. In the depth-weighting method, the weighting function is arbitrary as long as it varies the weights to the gradient with the depth.

The third method stems from the structure of the Hessian. It is well known that the Gauss-Newton method has a better convergence rate than the gradient-based method. However, it is quite expensive to calculate the Hessian matrix. In the frequency domain, Pratt et al. (1998) showed that the approximate Hessian is dominated by its diagonal terms. If neglecting the off-diagonal term of the approximate Hessian and assuming the inner product of the Green's functions are the same, Shin et al. (2001) concluded that the reversal of the diagonal of their pseudo-Hessian can compensate for the geometrical spreading. Choi et al. (2008) introduced the sum of the amplitudes of the impulse responses to the diagonal terms of the pseudo-Hessian. However, this new pseudo-Hessian only accounts for the geometrical spreading effect from the sources.

In full-waveform inversion, the amplitudes of both forward propagating waves from sources and backward propagating waves from receivers change with time and space during propagation. The Hessian depends on both wavefields from sources and receivers. We propose a new full-waveform inversion approach in the time domain that uses both the energies of forward and backward propagation waves to weight the gradient. It can effectively removes the effects of wave propagation from both sources and receivers, including transmission, scattering and geometrical spreading. We numerically demonstrate that the full-waveform inversion with energy-weighted gradients can enhance the convergence rate and particularly improve the reconstruction of the deep region of the model.

ENERGY-WEIGHTED GRADIENT

Full-waveform inversion in the time domain minimizes the misfit function given by

$$E = \sum_{(s,r)} \frac{1}{2} [\tilde{\mathbf{u}}(\mathbf{x}_r, \mathbf{x}_s) - \tilde{\mathbf{d}}(\mathbf{x}_r, \mathbf{x}_s)]^T [\tilde{\mathbf{u}}(\mathbf{x}_r, \mathbf{x}_s) - \tilde{\mathbf{d}}(\mathbf{x}_r, \mathbf{x}_s)], \quad (1)$$

where $\tilde{\mathbf{u}}$ is the synthetic wavefield at receiver r from source s , $\tilde{\mathbf{d}}$ is the data at receiver r from source s , and the superscript T represents the transpose.

The Hessian matrix is given by

$$\mathbf{H} = \tilde{\mathbf{A}}^T \tilde{\mathbf{A}} + \left(\frac{\partial \tilde{\mathbf{A}}}{\partial \mathbf{m}} \right)^T \delta \tilde{\mathbf{d}}, \quad (2)$$

Full-waveform inversion with an energy-weighted gradient

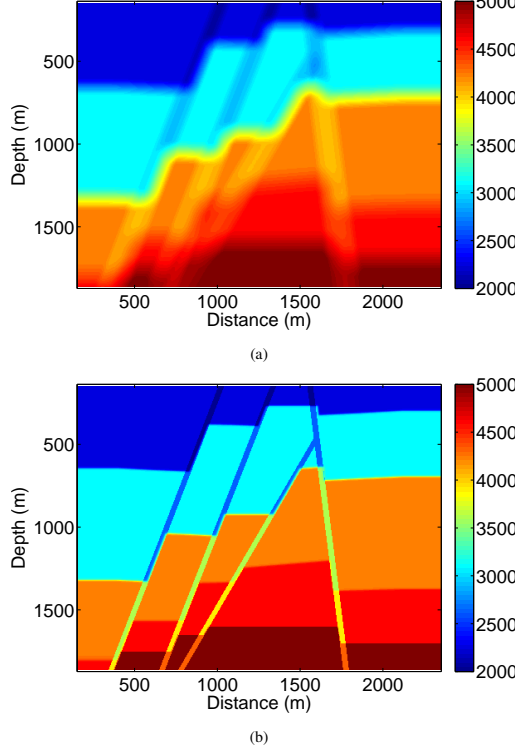


Figure 1: A velocity model with steep faults. (a) Smoothed initial velocity model for waveform inversion; (b) True velocity model (Courtesy of John Queen of Hi-Q Geophysical Inc.).

where \mathbf{m} is the model parameter and $\delta\tilde{\mathbf{d}} = \tilde{\mathbf{u}} - \tilde{\mathbf{d}}$. If the bulk module is the model parameter and the density is constant, the term $\tilde{\mathbf{A}}$ in equation (2) is given by

$$\tilde{\mathbf{A}} = \sum_{(s,r)} \nabla \cdot \mathbf{g}(\mathbf{x}, \mathbf{x}_r) * \nabla \cdot \mathbf{u}(\mathbf{x}, \mathbf{x}_s). \quad (3)$$

The approximate Hessian is simply $\mathbf{H}_a = \tilde{\mathbf{A}}^T \tilde{\mathbf{A}}$.

The term $\tilde{\mathbf{A}}$ has a dimension of $N \times M$, where N is the number of temporal data points and M the number of model parameters. Let $\mathbf{U}(\mathbf{x}, \mathbf{x}_s)$ be a discretized time series of $\nabla \cdot \mathbf{u}(\mathbf{x}, \mathbf{x}_s)$, and $\mathbf{G}(\mathbf{x}, \mathbf{x}_r)$ be a discretized time series of $\nabla \cdot \mathbf{g}(\mathbf{x}, \mathbf{x}_r)$, then the diagonal terms of the approximate Hessian becomes

$$\text{diag}\{\tilde{\mathbf{A}}^T \tilde{\mathbf{A}}\} = \left\{ \sum_{(s,r)} [\mathbf{U}^T(\mathbf{x}_1, \mathbf{x}_s) \mathbf{G}(\mathbf{x}_1, \mathbf{x}_r)]^2 \right. \\ \left. \dots \sum_{(s,r)} [\mathbf{U}^T(\mathbf{x}_M, \mathbf{x}_s) \mathbf{G}(\mathbf{x}_M, \mathbf{x}_r)]^2 \right\}. \quad (4)$$

Equation (4) clearly shows that it contains wave propagation effects from both sources and receivers. Equation (4) is computationally expensive. To account for wave propagation effects, we use the forward and backward propagated wavefields to compute weights W_s and W_r :

$$W_s \equiv \sum_s \mathbf{U}^T(\mathbf{x}, \mathbf{x}_s) \mathbf{U}(\mathbf{x}, \mathbf{x}_s), \\ W_r \equiv \sum_r \delta\tilde{\mathbf{d}}^T \mathbf{G}^T(\mathbf{x}, \mathbf{x}_r) \mathbf{G}(\mathbf{x}, \mathbf{x}_r) \delta\tilde{\mathbf{d}}, \quad (5)$$

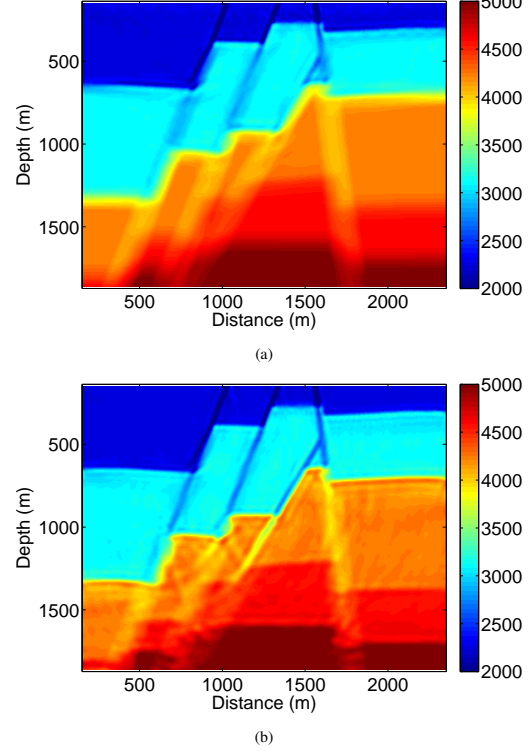


Figure 2: Results of full-waveform inversion with 10 iterations using the conjugate gradient method (a) and our new energy-weighted gradient method (b). The faults and the deep region in (b) are better reconstructed than those in (a).

and then obtain the energy-weighted gradient given by

$$\gamma_w = \frac{\tilde{\mathbf{A}}^T \delta\mathbf{d}}{W_s W_r}. \quad (6)$$

We use equation (6) to update the model during the full-waveform inversion.

In contrast, the pseudo-Hessian method in the frequency domain uses only the forward propagating wavefields from sources to weight the gradient (Choi et al., 2008). The diagonal terms of the approximate Hessian in the frequency domain are given by (Pratt et al., 1998)

$$\text{diag}(\mathbf{H}_a) = \sum \text{Re}\left\{ \left(\frac{\delta\mathbf{u}}{\delta m_1} \right)^T \left(\frac{\delta\mathbf{u}}{\delta m_1} \right)^* \right. \\ \left. \left(\frac{\delta\mathbf{u}}{\delta m_2} \right)^T \left(\frac{\delta\mathbf{u}}{\delta m_2} \right)^* \dots \left(\frac{\delta\mathbf{u}}{\delta m_M} \right)^T \left(\frac{\delta\mathbf{u}}{\delta m_M} \right)^* \right\}, \quad (7)$$

where

$$\text{Re}\left\{ \left(\frac{\delta\mathbf{u}}{\delta m_i} \right)^T \left(\frac{\delta\mathbf{u}}{\delta m_i} \right)^* \right\} = (\mathbf{f}_i)^T (\mathbf{S}^{-1})^T (\mathbf{S}^{-1})^* (\mathbf{f}_i)^*. \quad (8)$$

In equation (8), \mathbf{S} is the complex impedance matrix, and \mathbf{f}_i the virtual source vector. To simplify the calculation, Choi et al. (2008) defined a new pseudo-Hessian as:

$$\text{diag}\{(\mathbf{H})_{\text{new-}p}\} = \sum \text{Re}\{(\mathbf{f}_{s,1})^T \mathbf{A}(\mathbf{f}_{s,1})^* \dots (\mathbf{f}_{s,M})^T \mathbf{A}(\mathbf{f}_{s,M})^*\}, \quad (9)$$

Full-waveform inversion with an energy-weighted gradient

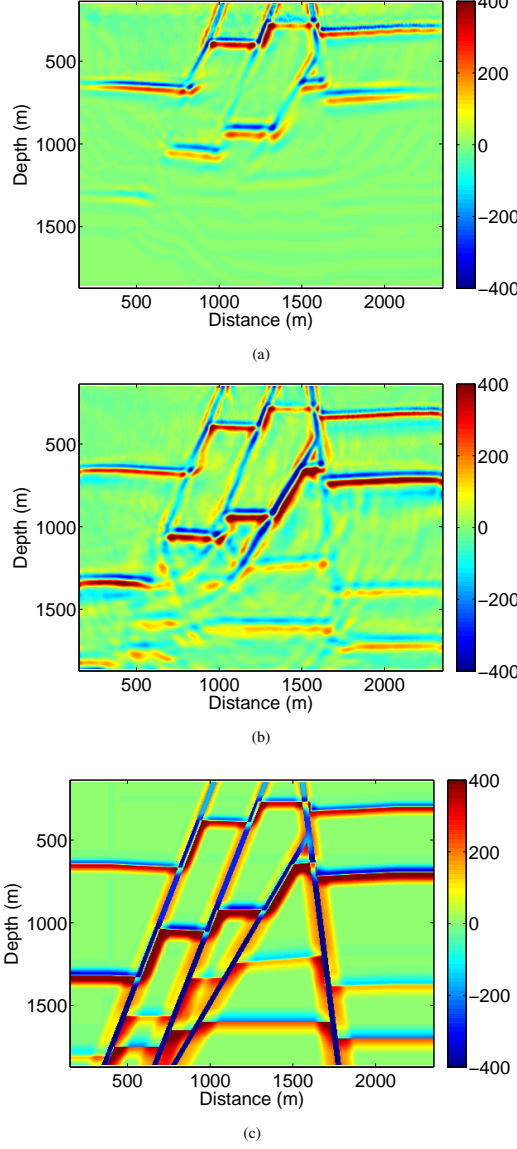


Figure 3: The panels in (a) and (b) are the differences between the inversion results in Fig. 2 and the initial smoothed model in Fig. 1(a), and the panel in (c) is the true difference between Fig. 1(b) and Fig. 1(a). The faults and the deep region are better reconstructed by our energy-weighted gradient method (b) than the conjugate gradient method (a).

with

$$\text{diag}\{\mathbf{A}\} = \text{Re}\left\{\sum_{s=1}^{n_s} |g_{s,1}| \cdots \sum_{s=1}^{n_s} |g_{s,2n}|\right\}, \quad (10)$$

where g is the impulse response, n_s is the number of sources, and n is the number of model grid points. Using equation (10) compensates for the geometrical spreading effect only from sources, not from receivers.

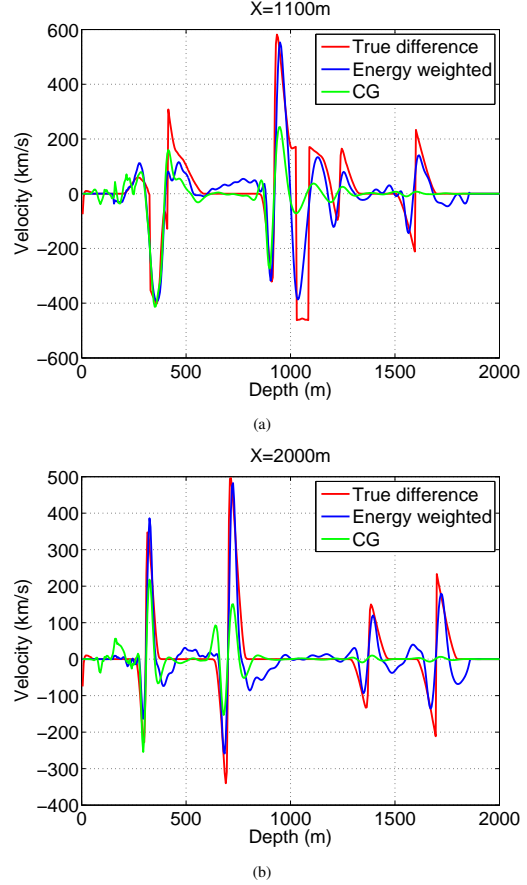


Figure 4: Two vertical profiles of Fig. 3 at two horizontal positions of (a) $X=1100$ m and (b) $X=2000$ m.

NUMERICAL RESULTS

We use a model with several steep faults as shown in Fig. 1 to test and verify the improved capability of the full-waveform inversion with our new energy-weighted gradient method for reconstructing the steep faults and the deep region of the model. We generate synthetic reflection data for 20 sources and 450 receivers located on the top surface of the model. The central frequency of the source wavelet is 25 Hz. Figure 2 shows the results obtained using the conjugate gradient (CG) method and our energy-weighted gradient (EWG) method. The differences between the reconstructed images and the initial model are displayed in Fig. 3. Figs. 2 and 3 clearly show that, while the CG method can reconstruct only the shallow region of the model, the EWG method can recover both the shallow and deep regions, and can reconstruct the steep faults better than the CG method. Comparing the shallow region above the depth at 800 m in Figs. 3(a) and (b), we can see that the EWG method reconstructs the model better than the CG method.

Figure 4 shows a comparison of the two vertical profiles of Fig. 3 at two horizontal positions of 1100 m and 2000 m. In the region beneath about 1000 m in Fig. 4(a), the reconstruction result of the EWG method is significantly better than that of

Full-waveform inversion with an energy-weighted gradient

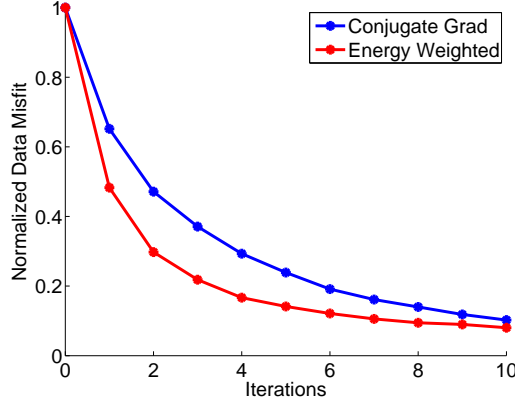


Figure 5: Comparison of the data misfits of the CG and EWG methods as a function of iterations. The misfit of the EWG method decreases faster than that of the CG method.

the CG method. For the vertical file in Fig. 4(b), the EWG method greatly improves the reconstruction from the depth at approximately 300 m to the bottom of the model compared to the CG method. Note that only 20 common-shot gathers are used in this study. The EWG results will be further improved by using more common-shot gathers of data.

Figure 5 is a comparison between the data misfits of the EWG and CG methods as a function of iterations. The data misfit of the EWG method decreases more rapidly than that of the CG method in the first a few iterations, which proves that weighting using the uneven spatial distribution of acoustic-wave energy plays an important role in full-waveform inversion. Figure 5 shows that the misfit of the CG method is almost the same as that of the EWG method after 10 iterations, even though the reconstructed model of the CG method still significantly differs from the true model (see Fig. 2a and the green line in Fig. 4). This is because the early arrivals in the data, or reflections from the shallow region of the model, contain much stronger wave energy than the later arrivals, and dominate the value of the data misfit function.

The pseudo-Hessian method developed by Choi et al. (2008) also accelerates the convergence of the gradient-based method. Fig. 6 shows that our energy-weighted gradient method gives a better balance of the gradient in shallow and deep regions compared to both the CG and pseudo-Hessian methods. Therefore, our EWG method can achieve a higher convergence rate for the entire model than the other methods.

CONCLUSIONS

We have developed an energy-weighted gradient method for full-waveform inversion in the time domain. The method accounts for the propagation effects of wavefields from both sources and receivers, and use the wave energies from sources and receivers to weight the gradient. We have numerically demonstrated that the energy-weighted gradient method significantly improves the reconstructions of both the shallow and deep regions of the model, and enhance the convergence rate of gradient-

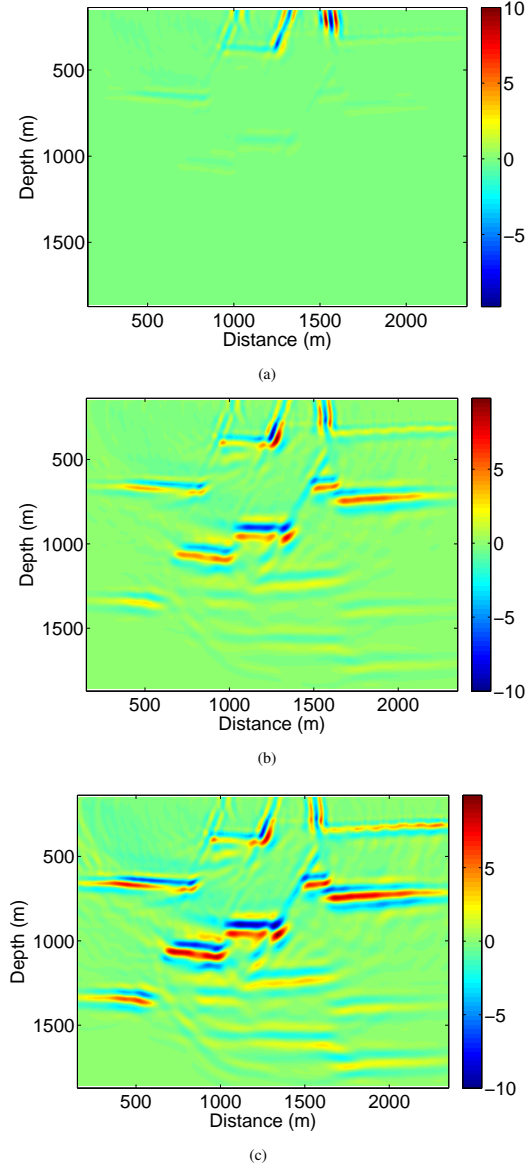


Figure 6: The gradients of the first iteration for (a) the conjugate gradient method, (b) the modified pseudo-Hessian method of Choi et al. (2008), and (c) our energy-weighted gradient method. Almost all the features in the model differences are more strongly enhanced by the EWG method, particularly the deep region of the model.

based methods without increasing computational cost.

ACKNOWLEDGEMENTS

This work was supported by U.S. DOE through contract DE-AC52-06NA25396 to Los Alamos National Laboratory. We thank John Queen of Hi-Q Geophysical Inc. for providing the model with steep faults.

Full-waveform inversion with an energy-weighted gradient

REFERENCES

Brenders, A. J., and R. G. Pratt, 2007, Full waveform tomography for lithospheric imaging: results from a blind test in a realistic crustal model: *Geophysical Journal International*, **168**, 133–151.

Choi, Y., D. J. Min, and C. Shin, 2008, Frequency-domain elastic full waveform inversion using the new pseudo-hessian matrix: Experience of elastic marmousi-2 synthetic data: *Bulletin of the Seismological Society of America*, **98**, 2402–2415.

Pratt, R. G., C. Shin, and G. J. Hicks, 1998, Gauss-newton and full newton methods in frequency-space seismic waveform inversion: *Geophysical Journal International*, **133**, 341–362.

Shin, C., K. Yoon, K. J. Marfurt, K. Park, and D. Yang, 2001, Efficient calculation of a partial-derivative wavefield using reciprocity for seismic imaging and inversion: *Geophysics*, **66**, 1856–1863.

Wang, Y., and Y. Rao, 2009, Reflection seismic waveform tomography: *Journal of Geophysical Research*, **114**, B03304.